



# Thermoelectric Higher Manganese Silicide: Synthetized, sintered and shaped simultaneously by selective laser sintering/Melting additive manufacturing technique

Yohann Thimont<sup>a,\*</sup>, Lionel Presmanes<sup>a</sup>, Vincent Baylac<sup>a</sup>, Philippe Tailhades<sup>a</sup>, David Berthebaud<sup>b</sup>, Franck Gascoin<sup>b</sup>

<sup>a</sup> CIRIMAT, Université de Toulouse, CNRS, INPT, UPS, 118 Route de Narbonne, F-31062 Toulouse Cedex 9, France

<sup>b</sup> Laboratoire CRISMAT UMR 6508 CNRS ENSICAEN, 6 boulevard du Maréchal Juin, 14050 Caen Cedex 04, France



## ARTICLE INFO

### Article history:

Received 2 November 2017

Received in revised form 2 December 2017

Accepted 6 December 2017

Available online 7 December 2017

### Keywords:

Additive manufacturing

SLS/SLM

HMS synthesis

Thermoelectric

## ABSTRACT

Complex geometry legs were advantageous to obtain higher thermoelectric potential due to a better thermal dissipation. Among all industrial processes, additive manufacturing using a selective laser sintering (SLS) or melting (SLM) techniques is the most promising to obtain such complex-shape legs without machining step. In this work, for the first time, Higher Manganese Silicide (HMS) sheet samples were synthesized, sintered and shaped simultaneously by additive manufacturing from ball milled manganese and silicon powder. Impact of surface power density and scanning rate of the laser on the microstructural and structural properties was discussed for some SLS/M parameters. Characterizations have shown that both densification and pure HMS phase can be obtained by SLS/M.

© 2017 Elsevier B.V. All rights reserved.

## 1. Introduction

Today, the market of the thermoelectric power generation for waste recovery in automotive, spatial and military applications is emerging. It should reach 610 M\$ in 2021 [1]. The p-type  $\text{MnSi}_y$  ( $1.7 < y < 1.8$ ) Higher Manganese Silicide (HMS) compound is a promising candidate for future thermoelectric (TE) applications in particular for TE modules in the 500 to 800 K range [2,3]. Y. Miyazaki et al. have described the crystal structure of HMS material by means of the (3 + 1)-dimensional superspace group approach [4]. Accordingly, all the HMS formulas can be treated as a single compound  $\text{MnSi}_y$ , where the [Mn] and [Si] are arranged in a tetragonal subsystem with the space groups of  $I4_1/amd$  and  $P4/nnc$ , respectively. This thermoelectric safe, green, and chemically stable material is made of non-rare and cheap elements. A lot of studies reported its TE properties for various dopants [5–12]. HMS have a low density ( $5.15 \text{ g/cm}^3$ ) which is crucial for TE applications in embedded devices [13,14] and are considered as promising TE material from industrial point of view [15]. Nevertheless, the synthesis of HMS legs stays difficult at an industrial scale because HMS is hard [16]. A lot of experimental techniques have been employed in the literature for TE silicide compounds

synthesis [17], [14]. HMS are commonly sintered by hot pressing or Spark Plasma Sintering techniques [18]. However, these techniques are not adapted to fabricate very complex shapes parts and the total cost of legs production remains expensive. The present work brings information about further eventual feasibility of HMS legs directly manufactured from a mixture of its precursors by additive manufacturing technique. TE devices with new geometries are of great interest for the thermal energy harvesting optimization [19]. Today, Selective Laser Sintering (SLS) or melting (SLM), is an emerging technology and seems to be the best way to make TE legs with complex geometries [20]. However, this technique is mainly used for structural materials (steel, titanium, aluminum, polymers) without additional interests to their electronic properties. First success of thermoelectric materials sintering using laser has been reported for  $\text{Bi}_2\text{Te}_3$  [21,22]. Nevertheless,  $\text{Bi}_2\text{Te}_3$  has not been synthesized from a mixture of its elementary constituents. In this study, SLS/M technique [23] has been carried out using a powder mixture based on its precursors. The basic idea was to demonstrate the simultaneously HMS material synthesis and sintering by SLS technique for an eventual further legs preparation. Powder consumption in SLS is usually very important, in the present work we made feasibility experiments with a small amount of precursor powder in alumina support.

\* Corresponding author.

E-mail address: [thimont@chimie.ups-tlse.fr](mailto:thimont@chimie.ups-tlse.fr) (Y. Thimont).

**2. Experimental**

Commercial manganese and silicon powders (Alfa Aesar 99.5%) have been mixed and ball milled (1 manganese for 1.95 silicon in atomic ratio) in a 20 mL ball milling device with 10 balls of 10 mm diameter then milled at 450 rpm for  $2 \times 10$  min. The precursor powder has been characterized by X-Ray Diffraction (BRUKER D8) in  $\theta$ - $2\theta$  mode and Scanning Electronic Microscope (JEOL JSM – 6400). The experiments were carried out with a SLS/M ProX 200 apparatus (wavelength: 1070 nm) which is perfectly adapted for metallic materials, therefore relatively well adapted to a Mn-Si

mixture. Precursor powder has been introduced in alumina cups then mechanically pressed under 28 kPa to reproduce the mechanical pressure applied by the SLS/MProX 200 machine before insolation. The chamber was inerted with argon to avoid oxidation. The laser scanning pattern was defined by a  $1 \times 1$  cm<sup>2</sup> square shape with only one pass. The spacing between the insolation lines (p) has been arbitrary fixed at 50  $\mu$ m. The studied SLS/M parameters were the laser power (P) established in the {30; 45} W range, laser spots diameters (D) of {420; 605}  $\mu$ m and the laser scanning rate (v) in the {50; 150} mm/s range. The energy dose ( $E_d$ ) received by the powder bed was calculated according to  $E_d = 4P/(\pi Dv)$ .

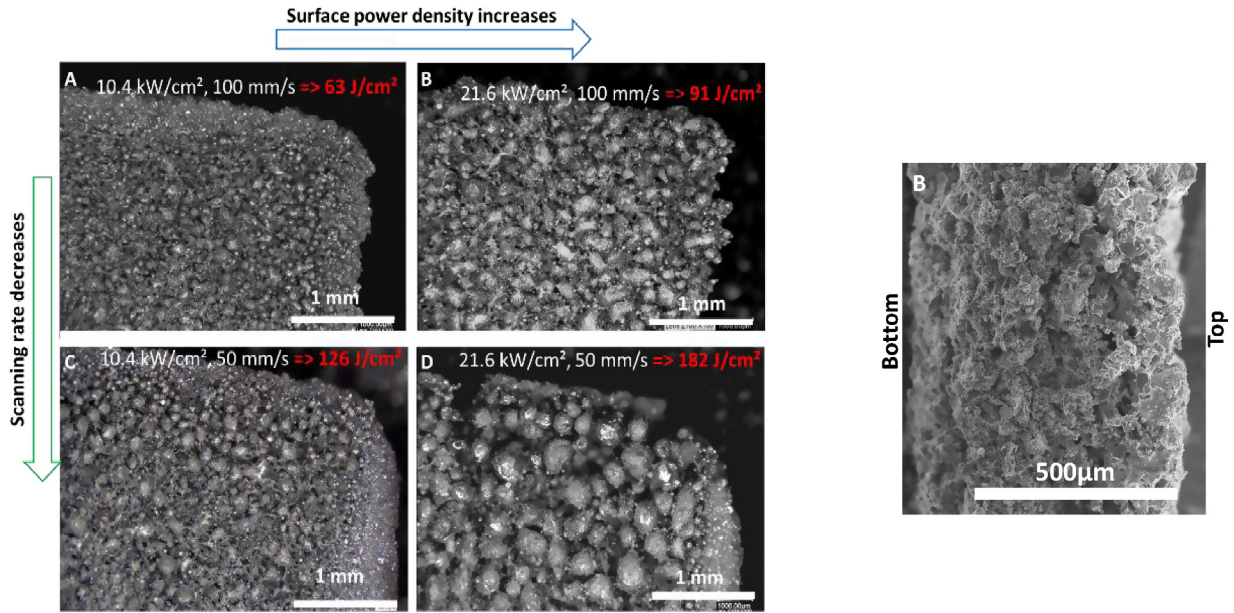


**Fig. 1.** (Left) optical micrographies of the surface of the sheet samples made under various SLS/M energy doses (J/cm<sup>2</sup>), Surface Power Density (kW/cm<sup>2</sup>), laser scanning rates (mm/s). (Right), a cross section of the sample B.

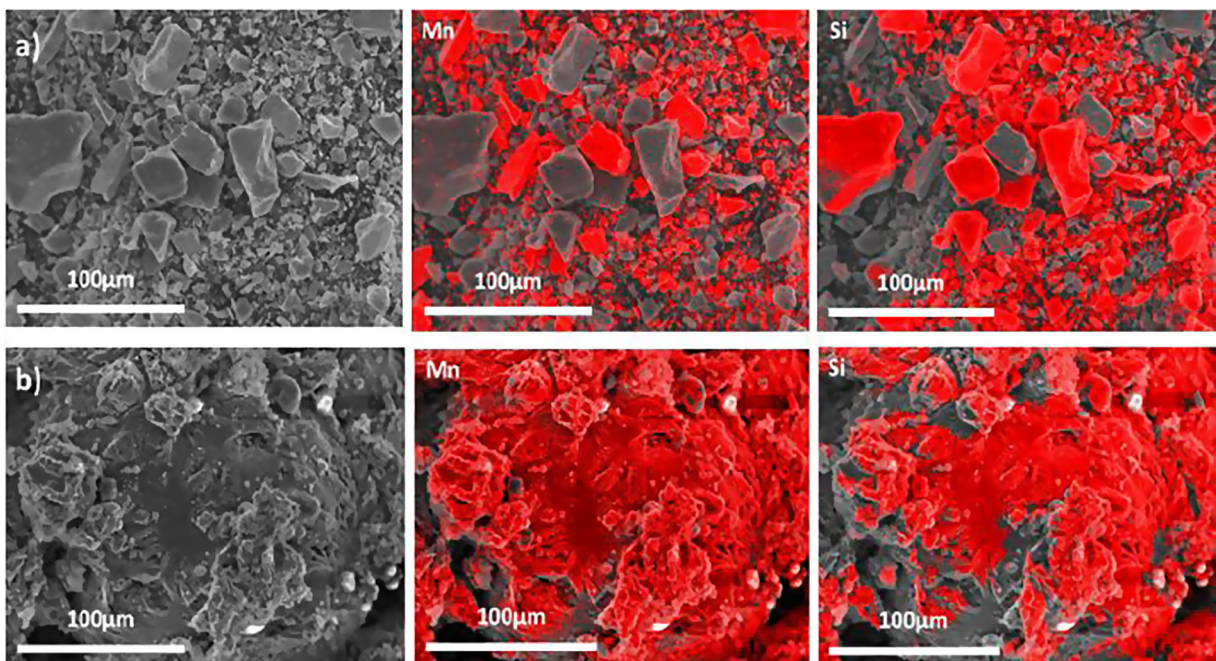


**Fig. 2.** SEM (Mode SE2) of (a) ball milled precursor powder (Mn and Si) and (b) Sample B manufactured by SLS/M, in right side the corresponding elements cartographies.



The samples with a sufficient mechanical cohesion were cleaned with pure ethanol in ultrasonic bath and dried under nitrogen flow. Only samples which have been manufactured with an  $E_d$  lying from 63 to 182 J/cm<sup>2</sup> could be handled and studied.

### 3. Results and discussion

The Fig. 1 shows for given SLS/M parameters (described for each micrograph obtained by a KEYENCE VHX microscope X100) the top view of main samples manufactured which have a sufficient mechanical cohesion and a representation of a sample B cross section. Optical micrographies were sorted according to the received energy doses which was increasing from the sample A to D. The sample A has been elaborated with an  $E_d$  of 63 J/cm<sup>2</sup>. It has a good homogeneity with small grains and its geometry was respected. Nevertheless, the sample was fragile probably because the energy dose was not sufficient to complete the powder sintering and reaction. The sample B prepared with an  $E_d$  of 91 J/cm<sup>2</sup> showed melted grains with good intergranular boundaries and a good surface homogeneity (typical of SLS/M process). The cross section shows homogenous microstructure along the depth. The over-melted balls grains start to appear in the case of sample C where the  $E_d$  was fixed to 126 J/cm<sup>2</sup> and become worst for the sample D which is mechanically brittle. It is mainly due to a thermal energy accumulation caused by the low thermal conductivity. We have concluded that the  $E_d$  of 126 J/cm<sup>2</sup> was too high. For these reasons, only samples A and B were selected for complementary analysis. Sample surfaces are rough even for optimized  $E_d$ , this is mainly due to the use of precursor powder whose grain size and shape are not well adapted to the SLS process. A SEM micrograph is reported in the Fig. 2 (bottom) and is compared with the precursor powder (top). Observation of sample B surface showed joined grains revealing the presence of a sintering mechanism. The sample B has been analyzed by elements cartography technique (Fig 2 - right). The microstructure consists of very large grains in comparison with the starting powder suggesting grain growth mechanism induced by the laser heating. Distribution of the elements in the grains in the sample B appears homogeneous in agreement with an alloy formation.

The XRD diagrams of the sample A and B are reported in the Fig. 3 (center). The sample B showed mainly MnSi<sub>y</sub> phase (JCPDS 01-072-7484) and proves that the reaction between the manganese and the silicon can be initiated by a laser while those of sample A have shown only a small amount of HMS phase esti-

ated at 44% in volume (by Gwyddion image analysis software) due to a lack of applied energy dose to complete the reaction. Samples C and D were too brittle and have not allowed to made XRD analysis. The experimental lattice tetragonal parameters are  $a = 5.528 \text{ \AA}$  and  $c = 17.478 \text{ \AA}$ . The influence of the energy dose is crucial to obtain the HMS phase and sintering.

### 4. Conclusions

In our study, HMS material synthesized and sintered directly from ball milled manganese and silicon powders by SLS/M has been demonstrated. An energy dose of 91 J/cm<sup>2</sup> allowed to obtain the MnSi<sub>y</sub> phase and its sintering. Results presented here are innovating and provide a foundation for future work to investigate the manufacturability of HMS in a layer-by-layer process using SLS/M technique to conceive appropriate legs geometries adapted to specific applications. The total cost of the HMS legs fabrication could be reduced in comparison with the actual way of production thanks to its low energy needs and no materials discard. However, precursor powder should be optimized in size and shape to improve sample density and microstructure.

### Acknowledgments

The authors would thank the Cellule Energie program funded by the CNRS and Jean-Jacques DEMAI for SEM micrographies and Benjamin DUPLOYER for XRD.

### References

- [1] Zion Market Research, <http://www.zionmarketresearch.com>.
- [2] M.I. Fedorov, G.N. Isachenko, Silicides: materials for thermoelectric energy conversion, *Jpn. J. Appl. Phys.* 54, 07JA05.
- [3] X. She, X. Su, H. Du, T. Liang, G. Zheng, Y. Yan, R. Akram, C. Uher, X. Tang, High thermoelectric performance of higher manganese silicides prepared by ultra-fast thermal explosion, *J. Mater. Chem. C* 3 (2015) 12116–12122, <https://doi.org/10.1039/C5TC02837J>.
- [4] Y. Miyazaki, D. Igarashi, K. Hayashi, T. Kajitani, K. Yubuta, Modulated crystal structure of chimney-ladder higher manganese silicides MnSi<sub>γ</sub> ( $\gamma \sim 1.74$ ), *Phys. Rev. B*, 78(21) (2008) 214104–214112.
- [5] A. Nozariasbmarz, A. Agarwal, Z.A. Coutant, M.J. Hall, J. Liu, R. Liu, A. Malhotra, P. Norouzzadeh, M.C. Öztürk, V.P. Ramesh, Y. Sargolzaei Aval, F. Suarez, D. Vashaee, Thermoelectric silicides: a review, *Jpn. J. Appl. Phys.* 56 (2017) 05DA04, <https://doi.org/10.7567/JJAP.56.05DA04>.
- [6] W. Luo, H. Li, Z. Linuxuan, Q.X. Tang, Q. Zhang, C. Uher, Rapid synthesis of high thermoelectric performance higher manganese silicide with in-situ formed nano-phase of MnSi, *Intermetallics* 19 (2011) 404.
- [7] V. Ponnambalam, D.T. Morelli, S. Bhattacharya, T.M. Tritt, The role of simultaneous substitution of Cr and Ru on the thermoelectric properties of defect manganese silicides MnSi<sub>d</sub> ( $1.73 < d < 1.75$ ), *J. Alloys Compd.* 580 (2013) 598–603, <https://doi.org/10.1016/j.jallcom.2013.07.136>.
- [8] A.J. Zhou, T.J. Zhu, X.L.N. Zhao, S.H. Yang, T. Dasgupta, C. Stiewe, R. Hassdorf, E. Mueller, Improved Thermoelectric Performance of Higher Manganese Silicides with Ge Additions, *J. Electron. Mater.* 2010 (2002) 39.
- [9] X. Chen, A. Weaters, D. Salta, L. Zhang, J. Zhou, J.B. Goodenough, L. Shi, Phase Formation and Thermoelectric Properties of Doped Higher Manganese Silicides (Mn<sub>1.5</sub>Si<sub>2.6</sub>), *J. Appl. Phys.* 114 (2013), 173705. [10.1063/1.2214104](https://doi.org/10.1063/1.2214104)
- [10] D.Y. Nhi Truong, D. Berthebaud, F. Gascoin, H. Kleinke, Molybdenum, Tungsten, and Aluminium Substitution for Enhancement of the Thermoelectric Performance of Higher Manganese Silicides, *J. Electron. Mater.* 44 (2015) 3603–3611, <https://doi.org/10.1007/s11664-015-3854-x>.
- [11] M. Saleemi, A. Famengo, S. Fiameni, S. Boldrini, S. Battiston, M. Johnsson, M. Muhammed, M.S. Toprak, Thermoelectric performance of higher manganese silicide nanocomposites, *J. Alloys Compd.* 619 (2015) 31–37, <https://doi.org/10.1016/j.jallcom.2014.09.016>.
- [12] A. Yamamoto, S. Ghodke, H. Miyazaki, M. Inukai, Y. Nishino, M. Matsunami, T. Takeuchi, Thermoelectric properties of supersaturated Re solid solution of higher manganese silicides, *Jpn. J. Appl. Phys.* 55 (2016) 020301–20304.
- [13] J. Schiltz, M. Riffel, K. Pixius, H.J. Meyer, Synthesis of thermoelectric materials by mechanical alloying in planetary ball mills, *Powder Technol.* 105 (1999) 149–154.
- [14] T.-H. An, S.-M. Choi, W.-S. Seok, C. Park, I.-H. Kim, S.-U. Kim, Effects of Spark Plasma Sintering Temperature on Thermoelectric Properties of Higher Manganese Silicide, *J. Electron. Mater.* 42 (7) (2013) 2269–2273.
- [15] S. Leblanc, Thermoelectric generators: linking material properties and systems engineering for waste heat recovery applications, *Sustainable Mater. Technol.* 1 (2014) 26–35.

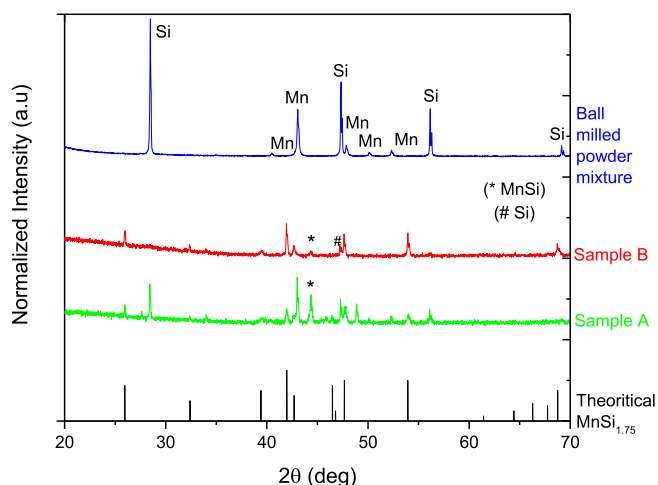


Fig. 3. XRD diagrams of ball milled precursors (top), samples A and B (center) and the HMS theoretical peaks for the composition MnSi<sub>1.75</sub> (bottom).

- [16] M.J. Yang, L.M. Zhang, L.Q. Han, Q. Shen, C.-B. Wang, *Indian J. Eng. Mater. Sci.* 16 (2009) 277–280.
- [17] L. Shi, J. Goodenough, M. Hall, J. Zhou, High-Performance Thermoelectric Devices Based on Abundant Silicide Materials for Vehicle Waste Heat Recovery, 2010 NSF/DOE Partnership on Thermoelectric Devices for Vehicle Applications.
- [18] C. Fanciulli, S. Battiston, S. Boldrini, E. Villa, A. Famengo, S. Fiameni, M. Fabrizio, F. Passaretti, Effect of Open Die Pressing on chemical-physical properties of  $Zn_4Sb_3$  compound, *Mater. Today Proc.* 2 (2015) 566–572.
- [19] A.Z. Sahin, B.S. Yilbas, The thermoelement as thermoelectric power generator: effect of leg geometry on the efficiency and power generation, *Energy Convers. Manage.* 65 (2013) 26–32.
- [20] W.A.W.K. Swainson, Method, medium and apparatus for producing three-dimensional figure product. US patent 4,041,476 (1977).
- [21] A. El-Desouky, M. Carter, M.A. Andre, P.M. Bardet, S. LeBlanc, Rapid processing and assembly of semiconductor thermoelectric materials for energy conversion devices, *Mater. Lett.* 185 (2016) 598–602, <https://doi.org/10.1016/j.matlet.2016.07.152>.
- [22] A. El-Desouky, M. Carter, M. Mahmoudi, A. Elwany, S. LeBlanc, Influences of energy density on microstructure and consolidation of selective laser melted bismuth telluride thermoelectric powder, *J. Manuf. Processes* 25 (2017) 411–417, <https://doi.org/10.1016/j.jmapro.2016.12.008>.
- [23] J.-J. Beaman, C.-R. Deckard, Selective laser sintering with assisted powder handling. US patent 4,938,816 (1990).